Title	Tuning the properties of PS-PIAT block copolymers and their assembly into polymersomes
Author(s)	Hans-Peter M. de Hoog; Dennis M. Vriezema; Madhavan Nallani; Suzanne Kuiper; Jeroen J. L. M. Cornelissen; Alan E. Rowan; Roeland J. M. Nolte
Citation	Hans-Peter, M. H., Dennis, M. V., Madhavan, N., Suzanne, K., Jeroen, J. L. M. C., Alan E. R., & Roeland, J. M. N. (2008). Tuning the properties of PS-PIAT block copolymers and their assembly into polymersomes. Soft matter, 4, 1003–1010.
Date	2008
URL	http://hdl.handle.net/10220/6789
Rights	

Tuning the properties of PS–PIAT block copolymers and their assembly into polymersomes†

Hans-Peter M. de Hoog,[a] Dennis M. Vriezema,[b] Madhavan Nallani,[a] Suzanne Kuiper,[a] Jeroen J. L. M. Cornelissen,*[a] Alan E. Rowan[a] and Roeland J. M. Nolte[a]

Received 17th October 2007, Accepted 4th February 2008
First published as an Advance Article on the web 4th March 2008
DOI: 10.1039/b716044e

The diblock copolymer polystyrene-*b*-polyisocyanoalanine(2-thiophene-3-yl-ethyl)amide (PS–PIAT) was prepared by reacting the isocyanide monomer (**1**) with a Ni(II) initiator complex prepared from polystyrene amine ($PS_{40}NH_2$), either obtained by atom transfer radical polymerization (ATRP) or anionic polymerization (AP). It was found that polymerization of optically pure **1** followed first-order kinetics in monomer concentration and resulted in the formation of insoluble block copolymers, whereas the rate of polymerization of optical mixtures of **1** was retarded and yielded block copolymers that were better soluble. Furthermore, PS–PIAT polymersomes of which the PS-block was prepared by AP were more stable than polymersomes of which the PS-block was prepared by ATRP, as was indicated by combined turbidity and dynamic light scattering (DLS) measurements on the aggregate solutions.

Introduction

In recent years block copolymers have received considerable attention as building blocks for the construction of well-defined nano-architectures by self-assembly.[1–3] In dilute solutions amphiphilic block copolymers can form different aggregate morphologies, *e.g.* micelles, vesicles, and helical structures depending on the type and the relative fraction of the constituting blocks.[4,5] Block copolymer based vesicles, also called polymersomes,[6–11] are promising self-assembled systems for which potential applications can be foreseen in drug delivery or as nano-sized reactors.[12,13] These vesicular structures are comparable to liposomes and cells in the sense that a water compartment is enclosed by a bilayer-like membrane but they are more robust than liposomes. On the other hand, the advantage of the biological lipid membrane is the fluidic structure that combines sufficient stability with flexibility in order to perform highly diverse functions.[5] With respect to biological cells rigidity is offered by the extracellular matrix in which high molecular weight polysaccharides like cellulose play an important role.

From a technological point of view polymersomes are more attractive than liposomes because of the high stability and toughness of the membrane compared to the latter aggregates.[4] Furthermore, membrane thickness and morphology can be tuned by variation of the polymer molecular weight and the relative degree of polymerization of the constituent blocks.[14,15] In addition, the properties of polymersomes can be readily changed by varying the chemical structure of the polymer segments while the chemistry available is broad, as is exemplified by the large variety of block copolymer structures reported to date that self-assemble into vesicles.[10] Controlled delivery of drugs is a major goal as can be seen from the emerging number of publications on stimuli-responsive,[16–18] and biodegradable polymersomes.[19–21] This theme has been extended to the incorporation of proteins with specific functions by which the polymersomes can be transformed into smart capsules.[22–25] Systems that have been extensively studied are the polystyrene-*b*-poly(acrylic acid) (PS–PAA) block copolymers, having a glassy component, and more flexible polymers based on polyethylene oxide (PEO), like polybutadiene-*b*-poly(ethylene oxide) (PB–PEO). In particular, PEO-based block copolymers may have a great impact on the field of drug-delivery because of their biocompatibility. A notable triblock copolymer that has been shown to be compatible with membrane-spanning protein channels is poly(2-methyloxazoline)-*b*-poly(dimethylsiloxane)-*b*-poly(2-methyloxazoline) (PDMS–PMOXA–PDMS).[26]

One of the more complex systems is the vesicle architecture prepared from polystyrene-*b*-polyisocyanoalanine(2-thiophene-3-yl-ethyl)amide (PS-PIAT). In contrast to the above-mentioned polymersomes these polymers are able to assemble into vesicles which are porous to low molecular weight organic substances. Furthermore the thiophene functions in the PIAT headgroups can be polymerized after self-assembly, increasing the stability of the aggregates.[27] In this paper we present a thorough examination of the polymerization properties of PS–PIAT and their self-assembly conditions. An important factor was found to be the stereochemistry of the polyisocyanopeptide block, which determines the polymer solubility and related polymersome formation. In addition, the nature of the polystyrene-block turned out to influence the stability and morphology of the aggregates. Control over these parameters is crucial for the further development and application of this polymersome system in fields like biosensing and biotechnology.[28,29]

[a]*Institute for Molecules and Materials, Radboud University, Toernooiveld 1, 6525 ED, Nijmegen, The Netherlands*
[b]*Encapson BV, Toernooiveld 1, 6525 ED, Nijmegen, The Netherlands*
† Electronic supplementary information (ESI) available: Scheme S1, Fig. S1–S6 plus further experimental details. See DOI: 10.1039/b716044e

Results and discussion

Synthesis of block copolymers

The thiophene-containing isocyanoalanines were prepared *via* their corresponding formamides as is detailed in the ESI† (Scheme S1). Shortly, two batches of isocyano-L-alanine(2-thiophene-3-yl-ethyl)amide (**1**) were prepared, of which one batch was optically pure and one batch was partly racemized. Isocyanides can be polymerized in the presence of Ni(II) salts using an amine as the initiator.[30] For the preparation of block copolymers of **1** and PS, macromolecular initiator complexes obtained by reacting amino-terminated PS with the nickel salt of *tert*-butyl isocyanide were used (Scheme 1).[31,32] Polymerization of the isocyanide was initiated by adding the macromolecular initiator complex to a solution of **1**. The PS was obtained *via* two routes, *viz.* atom transfer radical polymerization (ATRP-PS) and anionic polymerization (AP-PS), resulting in diblock copolymers PS–PIAT **2** and **3** that differed slightly in the structure of the PS segment.

Polymerization of optically pure **1** initiated by either of the two initiator complexes proceeded rapidly and the reaction mixture became turbid within 5 minutes, indicating precipitation of the polymeric material from solution. Remarkably, reaction mixtures in which partly racemized **1** was used remained clear and consumption of monomer took at least 1 day.[33] To investigate the influence of the optical purity of the monomer on its rate of polymerization the polymerizations of enantiopure L-**1**, as well as a 75 : 25 and a 50 : 50 mixture of L-**1** to D-**1**, were studied by using 1 : 50 molar equivalents of the nickel complex prepared from ATRP-PS as initiator (Table 1).[31,32,34] The 75 : 25 mixture of monomers was also copolymerized with the initiator complex obtained from AP-PS, yielding **3**.

During the polymerization reaction, samples were taken at 1 hour intervals and the area of the isocyanide stretching

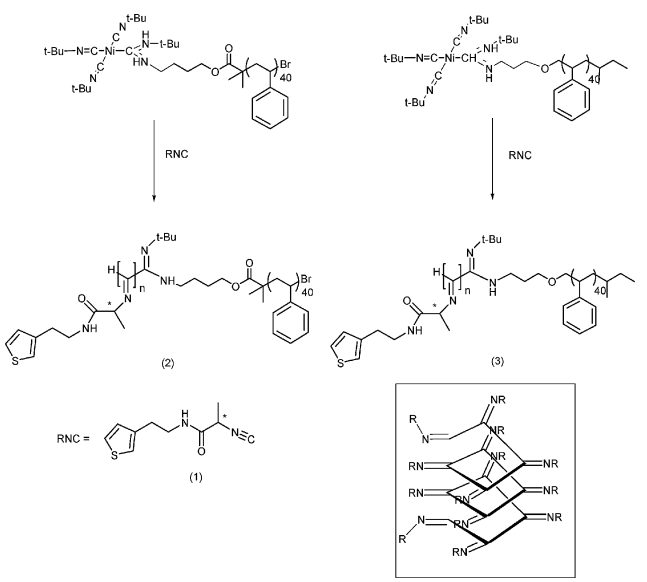

Scheme 1 Polymerization of isocyanide **1** with initiator complexes derived from PS obtained either *via* ATRP or *via* anionic polymerization. The structure in the square shows the helical fold of the isocyanide backbone and the resultant stacking of the side groups *n* and *n* + *4* above each other.

Table 1 Abbreviations and labels for the PS–PIAT diblock copolymers used in this study. The nature of the PS-block is indicated, as well as the ratio of enantiomers of isocyanide monomer **1** used in the polymerization reaction

Name	Label	PS obtained by	Ratio L-**1**/D-**1**
PS_{40}-*b*-$PIAT_n$ [a]	**2a**	ATRP	100 : 0
PS_{40}-*b*-$PIAT_n$	**2b**	ATRP	75 : 25
PS_{40}-*b*-$PIAT_n$	**2c**	ATRP	50 : 50
PS_{40}-*b*-$PIAT_n$	**3**	AP	75 : 25

[a] For synthesis and analysis details see experimental section.

vibration at 2139 cm^{-1} in the infra-red spectra was plotted *versus* time (Fig. 1A). The rate of polymerization of optically pure isocyanide obeyed first-order kinetics (k_p = 0.32 L mol^{-1} s^{-1}) up to a conversion of **1** of *ca.* 85% (Fig. 1B, open triangles), after which it deviated. A clear deviation from the first-order kinetics was observed in the block copolymerization experiments with mixtures of enantiomers (Fig. 1B, open circles and open squares). For both the 75 : 25 and 50 : 50 polymerizations the initial reaction rate appeared to be equal to that of the enantiopure **1**, but progressively slowed down during the reaction, reaching a final state after 24 hours. With respect to **2b** this point was reached at a monomer conversion of 75% and for **2c** at 45%. The enantiopurity of the sample apparently determines both the rate of the reaction and the conversion.

When monitoring the increase of the amide NH-stretching vibration in the IR-spectrum of **2b** and **2c** the same trend was observed, indicating that the formation of the helix occurred simultaneously with the incorporation of the isocyanide.[35] Remarkably, the plot for the increase in NH-stretch of **2a** did not show first-order kinetics but instead showed a similar trend as observed for the racemic monomer.

Upon polymerization, the amide vibrations of polymers **2a–c** showed large shifts to lower wave numbers, indicative of the formation of a hydrogen-bonding network.[34,36] The formation of H-bonds was also indicated by ^{1}H-NMR based on the observed large downfield shifts ($\Delta\delta_{NH}$ = 1.8 ppm) of the amide protons of the polymers. Interestingly, the IR-spectrum of **2a** displayed two peaks at 3325 and 3272 cm^{-1}, resulting from the hydrogen-bonded amide, whereas **2b** and **2c** showed a single broader peak around 3280 cm^{-1} (Fig. 2). Probably for the enantiopure polymer H-bonds cannot only form between residues *n* and *n* + 4 in the helix but also between other residues, like *n* + 3 or *n* + 5. For the amide I vibrations (ν = 1684 to 1654 cm^{-1}) the largest shift was observed for the polymers prepared from the (partly) racemic monomer, whereas the amide II shift (ν = 1529 to 1539 cm^{-1}) was largest for the optically pure polymer. Comparing these results with previously reported data on isocyanodipeptides, it appears that the PIAT block obtained from optically pure **1**, resembles more the poly(isocyanoalanyl-alanine)s (PIAA) with respect to the hydrogen-bonding network than the poly(isocyanoalanyl-glycine)s (PIAG). In this latter polymer H-bonds between side chains are only partially present.[37]

The Cotton effect at *ca.* 300 nm in the circular dichroism (CD) spectra of chiral polyisocyanides originates from the $n \rightarrow \pi^*$ transitions of the helically arranged backbone imine functions,

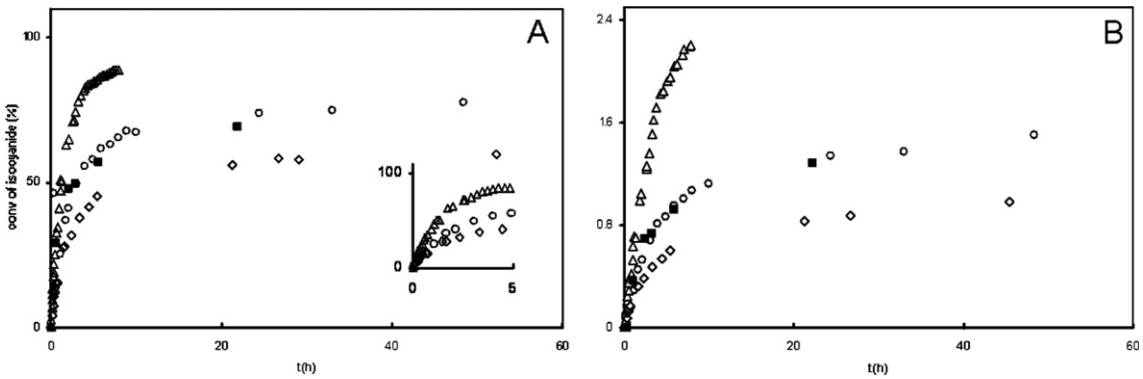

Fig. 1 Conversion of isocyanide **1** as a function of time (A) and the corresponding first-order rate plots (B). The polymerization of the optically pure isocyanide (Δ), as determined by following the CN stretching vibration in the IR, shows first-order kinetics. In the case of the mixtures of enantiomers of **1** (○ (75 : 25) and ◇ (50 : 50)) the rate of polymerization is markedly slowed down and is non-linear with respect to the monomer concentration. For each polymerization the initial concentration of isocyanide was 20 mM and the monomer to catalyst ratio was 50 : 1. The catalyst was prepared from ATRP-PS. Polymerization of isocyanide (75 : 25) initiated by the initiator complex obtained from AP-PS (■) is also shown. Inset: the initial 5 hours of the polymerization reaction.

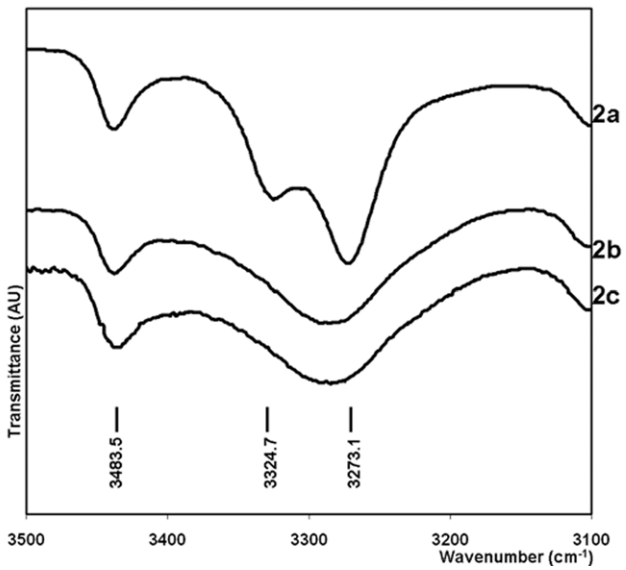

Fig. 2 IR-spectra in the region of the NH-stretching vibration of polymer samples of **2a–c** taken during polymerization from the reaction mixtures. Samples were taken after 2 hours and 12 hours for polymers **2a** and **2b,c** respectively. Free NH corresponding to the monomer is found at 3439 cm^{-1}. The NH-stretching vibrations of the polymers appear at lower wave numbers because they are involved in hydrogen-bonding. The enantiopure polymer shows two vibrations at 3325 and 3273 cm^{-1} likely originating from the hydrogen-bonded NH-group, whereas the (partly) racemized polymers show single, more broadened peaks at 3280 cm^{-1}.

which in some occasions is influenced by contributions from the chiral side chains.[38,39] The latter contributions often obscure the couplet typically observed for helical molecules.[40] For polyisocyanopeptides like L,L-PIAA, in which hydrogen-bonding arrays were shown to be present between side-chains n and $n + 4$ in the helix, a single intense Cotton effect centered around $\lambda = 315$ nm was observed, while for L-PIAG, which does not have well-defined hydrogen bonding arrays, a couplet with lower intensity was measured.[37] For the former polymer it was suggested that the ordering of the side chain amides is reflected in the imine $n \rightarrow \pi^*$ transitions. Because of the hydrogen bonds, the amide carbonyls in one particular array likely all point in the same direction and the resultant permanent dipole is expected to influence the nearby $n \rightarrow \pi^*$ transitions of the imine group considerably.[36]

Diblock copolymers of optically pure L-**1** and racemized **1** showed similar UV-spectra having a small shoulder as a result of the $n \rightarrow \pi^*$ transitions at approximately $\lambda = 290$ nm at the onset of a much more intense band in the far UV-region. This shoulder is responsible for the signals in the CD-spectrum in the range from $\lambda = 250$–500 nm; a broad negative Cotton effect with a maximum at $\lambda = 288$ nm was observed for all polymers (Fig. 3). Because the molecular weights of the polymers could not reliably be determined, the exact concentration of the diblock copolymer in solution was unknown (see below). The intensity of the CD-signal was therefore divided by the

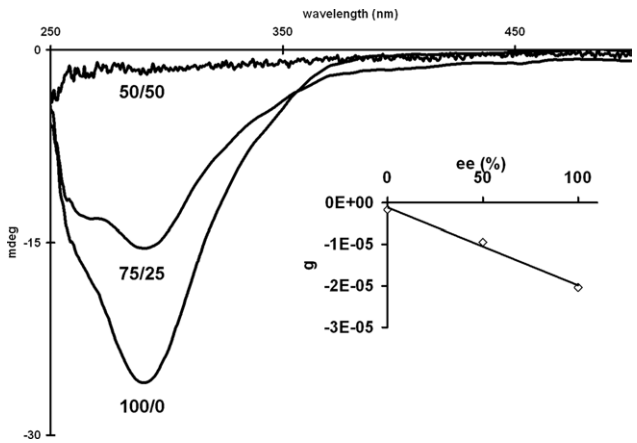

Fig. 3 CD spectra of block copolymers **2a**, **2b** and **2c**. Except for the intensity of the Cotton effect no difference was observed between **2a** on the one hand and **2b** and **2c** on the other hand. A plot of the normalized intensity, *g*, *versus ee* is shown in the inset indicating that the excess helix sense depends linearly on the ee of the monomer used.

absorbance to give the asymmetry factor, $g = \Delta\varepsilon/\Delta A$, which is independent of concentration.[41] The magnitude of g was found to depend linearly on the enantiomeric excess (*ee*) of the monomer used (Fig. 3, inset). This indicates that for the studied materials the optical purity of the monomers is directly transferred to the resulting polymers. No difference was observed between block copolymers of PS–PIAT in which the PS segment was obtained *via* ATRP or AP.

Although the IR data are in line with hydrogen-bonding between the side-chains of the PIAT-block, the CD-spectra suggest that the PIAT-blocks of **2a–c** have a less well-defined structure than the main chains of the previously studied polyisocyanopeptides.[35,36] Possibly, the kinetically determined structure of the helix that is formed, already during polymerization converts to a thermodynamically more stable one. This kind of process was also observed for polyiscyanodipeptides like PIAG,[42] and is similar to the unfolding known to occur in 'classic' polyisocyanides.[43] Polyisocyanides derived from β-amino acids were also reported to revert, on standing in solution, from a kinetically determined structure to a thermodynamically more stable one, as reflected in the CD spectra.[44] Interestingly, for these polymers it was observed that both the helical arrangement and the hydrogen-bonding network remained intact and only minor changes occurred in the corresponding spectra. For PIAG during polymerization, a transition was already observed to a state with only little secondary structure.[42]

Apart from its intensity, the enantiopure polymer **2a** showed the same CD-signal as the polymers prepared from a (partly) racemic monomer mixture, pointing to a similar structural organization of the helical polymer main chains. This is noteworthy, since **2a** precipitated during the reaction and the polymerization kinetics differed from those observed for **2b** and **2c**. Apparently, the solubility properties of the block copolymers, that are dictated by the PIAT segment, are related to the propagation rate of the polymerization reaction. Since the CD data and minor differences in the IR spectra suggest no outspoken structural differences, we tentatively conclude that a fast propagation reaction in the case of the monomer leading to **2a** yields an insoluble high molecular weight PIAT block. This is in line with the presence of free PS homopolymer in the material, even after full conversion of the monomer L-**1** (see below).

The polymerization rate of optically pure L-**1** is first-order in monomer concentration and the rate constant is calculated to be $k_p = 0.32$ L mol^{-1} s^{-1}. The presence of D-**1** in the reaction mixture, appears to hinder the incorporation of L-**1** into the growing helix, thereby slowing down the reaction rate. A reduced propagation rate compared to the initiation rate will result in shorter PIAT blocks with improved solubility. The presence of a chiral impurity therefore seems to be essential to the formation of the soluble di-block copolymers.

The retarded incorporation of L-**1** by its opposite stereoisomer is probably the result of steric interactions between the respective monomers when they coordinate simultaneously to the nickel center.[35,45,46] The chance of two monomers of opposite configuration coordinating to the nickel center is highest for the 50 : 50 polymerization, which showed the lowest polymerization rate (Fig. 1). During polymerization, either both enantiomers are incorporated into the same growing helix, or one particular enantiomer has first to be exchanged on the metal for its stereoisomer before inclusion in the growing chain is possible, after which the polymerization proceeds further. In both cases the rate of polymerization will be slowed down. The retarded incorporation of L-**1** into the growing helix in the presence of its enantiomer is reminiscent of the process described by Kamer *et al.*,[47] who found that one helix sense is preferred over the other when an achiral isocyanide is polymerized in the presence of an optically pure (slowly polymerizing) chiral isocyanide. Instead of the retarded incorporation of an achiral monomer by the presence of optically active isocyanide as in the case of Kamer *et al.*, the present polymerization of optically active isocyanide is retarded by the presence of its other enantiomer.

The polymerization reactions leading to **2b** and **2c**, show some resemblance with the polymerization of (pentamethyl phenyl)-ethyl isocyanide reported in the literature.[48] For this polymerization a slow initial polymerization was followed by a linear conversion of monomer in time. The kinetics could be described as first-order, but with a 'sliding' rate-constant (for formula see ESI†).[48,49] Applying this concept to the polymerization of the 50 : 50 mixture of L-**1**/D-**1**, the propagation rate is calculated to be $k_p = 0.07$ L mol^{-1} s^{-1}. For the 75 : 25 mixture, the calculated value is $k_p = 0.12$ L mol^{-1} s^{-1}. Extrapolation towards 100 % ee leads to a value of $k_p = 0.27$ L mol^{-1} s^{-1} for the polymerization of the enantiopure L-**1**. This is in reasonable agreement with the experimentally observed rate constant of $k_p = 0.32$ L mol^{-1} s^{-1}, suggesting that the propagation rate indeed varies linearly with the ee of the monomer.

In the case of (pentamethyl phenyl)ethyl isocyanide, it was suggested that the initiation rate compared to the polymerization rate was relatively slow.[48] As a result not all chains were initiated simultaneously, leading to a broad molecular weight distribution. Using GPC a broad molecular weight distribution was also found for the block copolymer **2b** (Fig. 4).‡ A significant signal with relatively low polydispersity was observed at longer elution times, corresponding to the polystyrene homopolymer (hPS). No difference was observed between polymers **2b** and **2c**

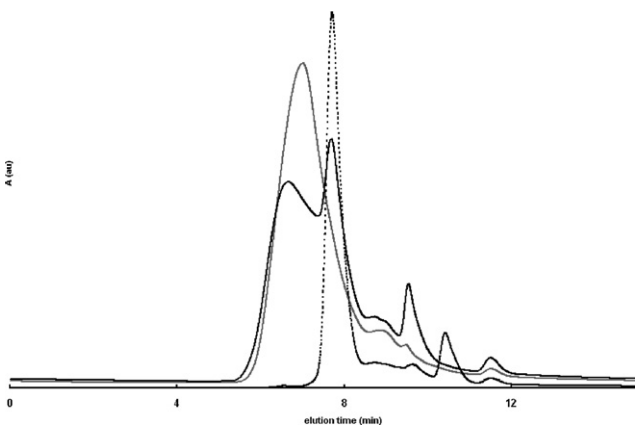

Fig. 4 GPC traces of PS–PIAT (**2b**, black trace) and (**3**, grey trace) of which the PS-block was obtained *via* ATRP and AP, respectively. The dashed line represents amino-terminated PS obtained by ATRP.

‡ Due to tailing the molecular weight distribution of polymer **2a** could not reliably be determined

(for **2c** see ESI†, Fig. S1). Interestingly, for **3** a broad unimodal distribution was observed with an M_n of 11 500 and a rather high polydispersity index of 2.2. Rather unexpectedly, as indicated by GPC, the AP-PS polymer used in the initiator complex behaved differently in the copolymerization reaction than the ATRP-PS polymer. This is remarkable since the kinetic analyses indicated no notable differences between reactions initiated with AP-PS–Ni(II) and ATRP-PS–Ni(II) complexes (Fig. 1).

The presence of homopolymer in the case of the polymerization with ATRP-PS–Ni(II) points to incomplete formation of the nickel carbene complex or to blocking of its catalytic activity in the polymerization reaction. Such inhibition could be the result of coordination of the carbonyl group in the linker of ATRP-PS to the nickel center, thereby hindering incoming monomers. Involvement of the bromine end-group of the ATRP-PS can not be excluded but seems to be more unlikely because of its distance from the nickel center. Partial and preliminary termination of the polymerization reaction may also explain the observed higher M_n for the PIAT block in the copolymer prepared with ATRP-PS (DP = 60, as estimated from ^{1}H-NMR) compared to the PIAT block in the copolymer obtained with AP-PS (DP = 25). The presence of homopolymer is not likely the result of incomplete end-group functionalisation of the polystyrenes used given the apparent purity of the amine terminated samples employed.

Aggregation behavior

As was previously shown, PS–PIAT diblock copolymers aggregate in a selective solvent to form polymersomes.[27] Since the optical purity of the monomer was found to influence the polymerization of the block copolymer (*vide infra*), it was reasoned that it might also have an effect on the aggregation behavior of the amphiphilic block copolymer. Indeed, transmission electron microscopy (TEM) analysis showed that when a diluted THF solution of **2a** was injected into water, only irregular aggregates were formed with no clear morphology. Block copolymers **2b** and **2c** both showed vesicular aggregates with diameters between 150 and 500 nm. No difference could be observed between block copolymers of differing optical purity, suggesting that not the optical activity, but merely the presence of a chiral impurity, and the resultant changes in block copolymer properties, influence the morphology of the formed assemblies.

An interesting observation was made for samples of **2b** from which the excess hPS (~40% w/w) was removed by precipitation, giving **2d**. Whereas **2b** showed vesicular aggregates with diameters ranging from 150–500 nm, the aggregates formed from **2d** were almost an order of magnitude smaller (50–80 nm) and had a more solid appearance (Fig. 5). The polymersomes observed for the native material, occasionally showed holes, in that way revealing their hollow interior. In contrast, the aggregates formed from the purified PS–PIAT looked more solid and had a uniform, reduced density under TEM, resembling micelles (ESI†, Fig. S2). Investigation of the structures formed in water by DLS revealed the presence particles with a mean radius of 200 nm after 24 h for dispersions of **2b** while dispersions of **2d** showed the presence of aggregates with a mean radius of around 80 nm (ESI†, Fig. S3) in the same time frame. For

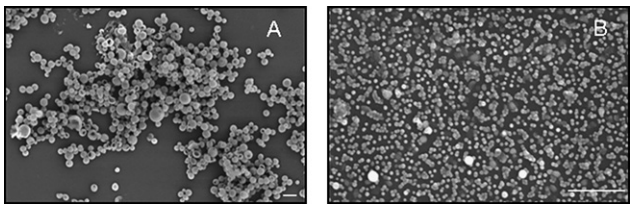

Fig. 5 SEM images of aggregates formed by injecting 0.5 ml of a 1.0 mg ml^{-1} THF-solution of PS–PIAT into 2.5 ml ultra-pure water (scale bar represents 1 μm). A) Polymersomes formed from **2b**. B) Monodisperse spheres of 50–80 nm in diameter formed from **2d**.

both polymers a similar trend is observed but the sizes deviate from electron microscopy measurements. This size difference is probably due to the effect of the polydispersity of the formed aggregates in the same way as described by Schmidt *et al.*[50]

It is known that the morphology of (block copolymer) vesicles can be influenced by varying the ratio of the two blocks or by varying external factors like pH, temperature and the addition of homopolymer.[8,10,11] Lu and Eisenberg showed that the morphology of PS–PAA aggregates could be changed from vesicles to micelles upon addition of hPS.[51] In that particular study, aggregation was induced by adding water to a DMF solution of the block copolymer. Under different aggregation conditions (*i.e.* by direct dissolution in DMF containing 7% water) the morphogenic effect observed upon the addition of hPS was clearly dissimilar.[52] The morphologies of block copolymer aggregates not always represent equilibrium structures,[7,53,54] but, in general, change from spheres to rods to vesicles and eventually to bilayers as the hydrophilic volume ratio is decreased. The micellar morphology seen for **2d** (Fig. 5), seems to be in accordance with what is expected for block copolymers with a relatively large headgroup. The presence of hPS will increase the hydrophobic volume, leading to a change in morphology from micelles to vesicles.

Polymersome stability

It was observed that without dialysis, polymersome solutions of **2** generally precipitated within 36 hours. Dispersions of **3** were found to be stable for at least 72 hours. Previously, it was shown that PS–PIAT polymersomes slowly increase in size by fusion of the vesicles over a period of 48 hours, after which a stable dispersion is obtained.[27] This growth coincided with an increase in turbidity of the polymer dispersions. To obtain a qualitative measure of the apparent difference in stability of the aggregates formed by polymers **2b** and **3**, self-assembly was induced by injecting THF solutions of the materials into water and subsequently measuring the turbidity at $\lambda = 660$ nm in time. At this wavelength the polymers only show minor absorbance and the observed increase in the optical spectra is attributed to a change in dimension or morphology of the aggregates.[55]

Mean turbidity values for 10 samples of hPS containing **2b** and **3** are shown in Fig. 6. For both polymers a 'lag time' during which the absorbance remained constant was observed (ESI†, Fig. S4). The graph clearly shows that the 'lag time' is longer (*i.e.* 12 h) for polymer **3**, after which the absorbance seems to increase and then to level off after 15 h. Eventually, after 20 hours, the turbidity again increased, concomitant with the

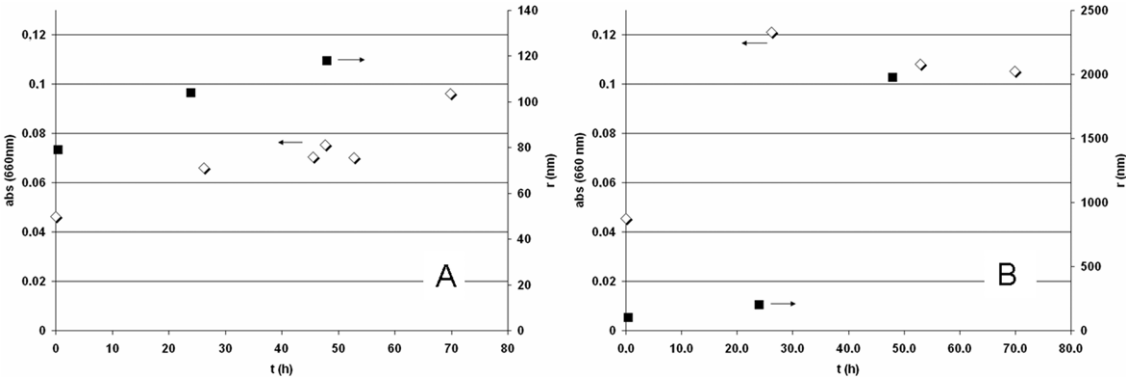

Fig. 6 Increase in absorbance at 660 nm and concomitant increase in radius for dispersions of polymer **3** (A) and polymer **2b** (B). Both polymers show a gradual increase in radius (■) in time but the increase for **3** is only minimal compared to polymer **2b**. In addition the maximum absorbance/turbidity (◇) for **2b** is already reached at 24 hours after which material gradually starts precipitating from solution.

appearance of a precipitate. This could be the result of the slow evaporation of the solvent. Indeed, the samples that were left open in air during the experiments showed a more distinct difference compared to samples that were measured in a sealed cuvette. Whereas in solutions of **2b** precipitation of material between 24 and 36 hours was observed in both cases, for polymer **3** this process was slower with minor precipitation occurring after 72 hours. In addition, the turbidity of aggregates formed by **3** was lower than that of **2b** at the same concentration, suggesting that there may be a difference in aggregate dimensions.

Samples were taken from the sealed vials after 0.5, 24 and 48 hours, and studied with DLS (Fig. 6 and ESI†, Fig. S5 and S6). The initial radius of the aggregates (at $t = 0.5$ h) was approximately equal for both polymers and rather small (~100 nm). After 24 hours, concomitant with the high turbidity of the dispersions, vesicles formed from **2b**, ranging in diameter between 150 and 500 nm as could be concluded from the EM and DLS data (Fig. 5). Vesicles of **3** had only increased to an average diameter of 120 nm and did not show any further increase in size after 48 hours. Although the turbidity of dispersions of **2b** remained constant after 48 hours DLS showed that the vesicles increased in size to an average diameter of 2 μm. Based on the above data, it seems that vesicles of **3** are smaller in size and more stable than vesicles formed from **2b**. Samples were taken from the sealed vials of samples **3** and **2b** after 24 hours, and studied by TEM (Fig. 7). Although both samples showed the presence of vesicular aggregates, vesicles of **3** appeared to be better-defined in shape and were more randomly distributed on the grid. Vesicles of **2b**, on the other hand, tended to cluster together and appeared more disperse in size and shape, tentatively explaining the observed difference in turbidity and the larger DLS based particle radius.

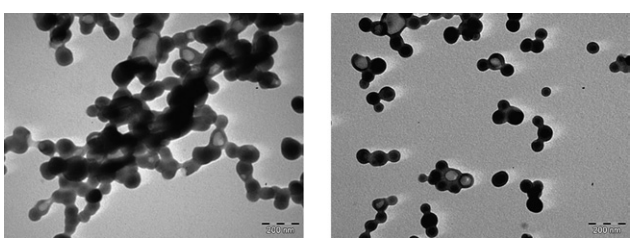

Fig. 7 Vesicular aggregates formed by injecting a 0.5 mg ml^{-1} THF solution of **2b** (left) and **3** (right) into ultrapure water. Both samples were taken from solutions with no precipitate in sealed vials after 24 hours standing.

Judged from the EM images, vesicles of **3** seem to be smaller with more consistent diameters of 150–200 nm.

The intrinsic instability of aggregates formed by polymers of **2b** is most likely the result of the excess of unreacted PS (40% w/w) present in the aggregates. Furthermore, as shown above, the presence of hPS affects the sizes of the aggregates formed. Because the hPS present is a result of an uncontrolled termination process of the PIAT polymerization the exact amount of hPS present in aggregates of **2b** could vary and consequently also lead to a variation in size of the vesicles among separate batches.

Experimental

Materials

Amine-functionalized polystyrene prepared by ATRP ($M_n = 4200$, PDI = 1.1) was obtained from Encapson B.V., Nijmegen, The Netherlands. PS–COOH prepared by anionic polymerization ($M_n = 4200$, PDI = 1.1) was bought from Polymer Source, Montreal, Canada, and converted to the PS–NH_2 by procedures described previously.[31] The conversions of the end-groups were followed by IR and were all quantitative. Block copolymerization experiments are described in Scheme 1, where ATRP-PS was used for the synthesis of block copolymer **2** and AP-PS for the synthesis of **3**. The isocyanide monomer was obtained *via* the procedure of Vriezema *et al.*,[56] except for the synthesis of boc-L-alanine(2-thiophene-3-yl-ethyl)amide (see ESI†, Scheme S1).

Synthesis of polystyrene-*b*-polyisocyanoalanine(2-thiophene-3-yl-ethyl)amide 2a–c

The polymerization was carried out as described previously.[55] For a given polymer the used enantiomer ratio of the monomers of **1** is indicated in Scheme 1. Except for the relative intensities of the protons on the polymer segments, the ^{1}H-NMR spectra of the products were the same. The degrees of polymerization

(DP) of the PIAT-blocks of **2a**, **2b** and **2c** could not be reliably estimated from their ^{1}H-NMR spectra because of the presence of hPS (up to 40%). Block copolymer **2b** was therefore repeatedly precipitated in petroleum ether 40–65 and from the purified fraction the DP of the PIAT-block was estimated to be 65. ^{1}H NMR (300 MHz, $CDCl_3$): δ = 8.1 (br, N*H*C(O)), 7.3–6.2 (br, CH*Ph*, thiophene H-5, thiophene H-4, thiophene H-2), 5.0–3.6 (br, C=NC*H*$(CH_3)_3$), 4.0–3.1 (br, thiophene-CH_2CH_2NH), 3.1–2.5 (br, thiophene-CH_2CH_2), 2.2–1.7 (br, CH_2CHPh), 1.7–0.9 (br, CH_2CHPh), 1.6–1.4 (br, CH(CH_3), 1.3–1.1 (C(CH_3)$_3$), 1.0–0.8 ppm (br, CH(Ph)C(CH_3)$_2$C(O). ^{13}C NMR ($CDCl_3$, 75 MHz): δ = 174–169 (N=C), 169–159 (NH*C*(O)), 145.2 (br, CHPh_{ipso}), 138.5 (br, thiophene C-3), 128–127 (br, CH$Ph_{ortho\ +\ meta}$, thiophene C-1 and thiophene C-2), 125.2 (br, CHPh_{para}), 120.7 (br, thiophene C-4), 67.8 (C(O)OCH_2), 62.4 (C=NC(CH$_3$)$_3$), 47–38 (br, *C*HPh and *C*H_2CHPh), 39.1 (br, CH_2CH_2NHC(O)), 38.3 (br, C(O)O$CH_2CH_2CH_2CH_2$NH), 31–29 (br, *C*H(CH_3)), 28.4 (*C*H_2CH_2NHC(O)), 25.1 (br, C(O)O$CH_2CH_2CH_2CH_2$NH), 23.0 (br, C(O)O$CH_2CH_2CH_2CH_2$NH) 22.6 (br, CH(Ph)C(*C*H$_3$)$_2$C(O) and 20.7 ppm (CH(*C*H$_3$). IR (**2a,** CH_2Cl_2, cm^{-1}) 3325 and 3272 (NH) 3092, 2979, 2936 and 2864 (CH), 1659 (amide I), 1602 (C=N), 1540 (amide II), 1494, 1453 (Ar C=C). IR (**2b,** CH_2Cl_2, cm^{-1}) 3285 (NH) 3092, 2979, 2936 and 2864 (CH), 1655 (amide I), 1602 (C=N), 1531 (amide II), 1494, 1453 (Ar C=C). IR (**2c,** CH_2Cl_2, cm^{-1}) 3281 (NH) 3092, 2979, 2936 and 2864 (CH), 1654 (amide I), 1602 (C=N), 1538 (amide II), 1494, 1452 (Ar C=C).

Synthesis of polystyrene-*b*-polyisocyanoalanine(2-thiophene-3-yl-ethyl)amide 3

The polymerization was carried out as described previously (see ESI†).[56]

General methods

Optical rotation. Optical rotation measurements were performed on a Perkin Elmer 241 polarimeter.

Chiral HPLC. Chiral HPLC was carried out using a Chiralpak AD chiral column and an UV-Vis detector operating at 250 nm. Hexane–2-propanol 8 : 2 (v/v) was used as eluent at a flow rate of 0.7 ml min^{-1}.

IR spectroscopy. IR spectra were acquired with a Bruker Tensor 27 FT-IR spectrometer fitted with a liquid cell. Samples (100 μl) were taken directly from the reaction mixture and directly used for measurement.

Gel-permeation chromatography. GPC was performed with a Shimadzu GPC with Shimadzu UV-Vis detector set at 254 nm and equipped with a Polymer Laboratories PL gel 5 μm mixed D-column and a PL 5 μm guard column (separation range: 500–300 000 molecular weight) using $CHCl_3$ as a mobile phase at 30 °C and running at 1 ml min^{-1}. PS standards were used for calibration.

Circular dichroism. CD spectra were recorded on a JASCO J-810.

Electron microscopy. For transmission electron microscopy and scanning transmission electron microscopy imaging respectively a JEOL JSM-6630F (60 kV) and JEOL JEM-1010 (12 kV) was used, both equipped with a CCD camera. Samples for TEM were prepared by drying a drop of an aqueous aggregate solution on a carbon-coated copper grid (Electron Microscopy Sciences, Hatfield, PA) and blotting away the excess water with a filter paper. No coating or staining was applied for TEM. SEM samples were prepared similarly, but the sample was coated by sputtering a 1.5 nm layer of Pd/Au with a Cressington 208 HR sputter coater fitted with a Cressington thickness controller.

Turbidity measurements. Turbidity experiments were performed in a 96-well plate using a Wallac Victor^2 1420 Multilabel Counter at 660 nm.

Dynamic light scattering. DLS experiments were carried out at the High Field Magnet Laboratory in Nijmegen with a home-built setup fitted with a Coherent CR599 dye laser operating at 600 nm. Samples, typically 1.5 ml, were prepared in a spherical glass cuvette and placed in a very stable and accurate thermostat set to 25 °C. Measurements were performed at an angle of 60° and the average hydrodynamic radius of the aggregates was calculated by CONTIN analysis.

Self-assembly. In a typical aggregation experiment, 0.5 ml of a 1.0 mg ml^{-1} solution of PS–PIAT in distilled THF was added drop wise to 2.5 ml of Milli-Q water. The solution was slowly shaken by hand to obtain a homogeneous solution.

Conclusions

In order to obtain a well-defined copolymer system suitable for future applications such as drug delivery and as nano-reactors, polymersome-forming block copolymers of polystyrene and a thiophene-containing isocyanopeptide were synthesized and their properties, in particular the aggregation behavior, studied. It was observed that two factors are of crucial importance for the formation of well-defined polymersomes from these block copolymers. First, the formation of soluble samples of PS–PIAT is determined by the optical purity of the starting monomer **1**. The presence of both enantiomers results in a decreased rate of polymerization of the PIAT-block compared to the optically pure monomer. The resulting block copolymer is soluble, whereas the polymerization of optically pure **1** occurs rapidly leading to polymer material that for the major part is insoluble. This difference in solubility is tentatively explained by the relatively high molecular weight of the enantiopure polymer.

Full initiation of **1** with the PS containing macro-initiators is found to depend on the nature of the PS block. AP-PS shows full conversion of the PS into the block copolymer, while samples of PS–PIAT initiated with ATRP-PS are found to contain a considerable portion of hPS. The exact nature of this difference is still under investigation, but interaction of functional groups (*e.g.* the carbonyl or bromide moieties) with the nickel center of the catalyst likely plays a role. The presence of the PS homopolymer appears to influence the aggregation of the block copolymers into polymersomes. Both types of PS–PIAT display

vesicle formation but polymersomes of PS–PIAT without hPS show enhanced stability in aqueous solution.

These results indicate that the chemistry and the aggregation behavior of PS–PIAT block copolymers is complex and highly dependent on the structure (*i.e.* composition, relative block length and (optical) purity of the constituting polymer blocks. Variations in this structure may lead to insoluble polymers or relatively unstable aggregates. Careful variation leads to polymers that assemble into well-defined and stable polymersomes. At present we are investigating the unique properties of these polymersomes further, in order to develop catalytically active capsules on the nano-scale.

Mr J. C. Gielen and Dr P. C. M. Christianen are acknowledged for the DLS studies. We thank Prof. I. W. C. E. Arends (Delft University of Technology) for fruitful discussions. The Research School NRSC-Catalysis, the Royal Netherlands Academy for Arts and Sciences, and the Chemical Council of the Netherlands Organization for Scientific Research are acknowledged for financial support.

References

1 I. W. Hamley, *Nanotechnology*, 2003, **14**, R39–R54.
2 T. P. Lodge, *Macromol. Chem. Phys.*, 2003, **204**, 265–273.
3 I. W. Hamley, *Angew. Chem., Int. Ed.*, 2003, **42**, 1692–1712.
4 H. Bermudez, A. K. Brannan, D. A. Hammer, F. S. Bates and D. E. Discher, *Macromolecules*, 2002, **35**, 8203–8208.
5 D. E. Discher and F. Ahmed, *Annu. Rev. Biomed. Eng.*, 2006, **8**, 323–341.
6 A. Mecke, C. Dittrich and W. Meier, *Soft Matter*, 2006, **2**, 751–759.
7 P. L. Soo and A. Eisenberg, *J. Polym. Sci., Part B: Polym. Phys.*, 2004, **42**, 923–938.
8 M. Antonietti and S. Förster, *Adv. Mater.*, 2003, **15**, 1323–1333.
9 B. M. Discher, Y. Y. Won, D. S. Ege, J. C. M. Lee, F. S. Bates, D. E. Discher and D. A. Hammer, *Science*, 1999, **284**, 1143–1146.
10 D. E. Discher and A. Eisenberg, *Science*, 2002, **297**, 967–973.
11 K. Kita-Tokarczyck, J. Grumelard, T. Haefele and W. Meier, *Polymer*, 2005, **46**, 3540–3563.
12 D. M. Vriezema, M. C. Aragonès, J. A. A. W. Elemans, J. J. L. M. Cornelissen, A. E. Rowan and R. J. M. Nolte, *Chem. Rev.*, 2005, **105**, 1445–1489.
13 J. A. Opsteen, J. J. L. M. Cornelissen and J. C. M. van Hest, *Pure Appl. Chem.*, 2004, **76**, 1309–1319.
14 Y. Yu, L. Zhang and A. Eisenberg, *Macromolecules*, 1998, **31**, 1144–1154.
15 O. Terreau, L. Luo and A. Eisenberg, *Langmuir*, 2003, **19**, 5601–5607.
16 O. Uzun, H. Xu, E. Jeoung, R. J. Thibault and V. M. Rotello, *Chem.–Eur. J.*, 2005, **11**, 6916–6920.
17 F. Chécot, S. Lecommandoux, H. A. Klok and Y. Gnanou, *Eur. Phys. J. E*, 2003, **10**, 25–35.
18 A. Napoli, M. J. Boerakker, N. Tirelli, R. J. M. Nolte, N. A. J. M. Sommerdijk and J. A. Hubbell, *Langmuir*, 2004, **20**, 3487–3491.
19 H. J. Lee, S. R. Yang, E. J. An and J. D. Kim, *Macromolecules*, 2006, **39**, 4938–4940.
20 F. Meng, G. H. M. Engbers and J. Feijen, *J. Controlled Release*, 2005, **101**, 187–198.
21 F. Ahmed and D. E. Discher, *J. Controlled Release*, 2004, **96**, 37–53.
22 C. Nardin, J. Widmer, M. Winterhalter and W. Meier, *Eur. Phys. J. E*, 2001, **4**, 403–410.
23 A. Ranquin, W. Versées, W. Meier, J. Steyaert and P. Van Gelder, *Nano Lett.*, 2005, **5**, 2220–2224.
24 H. J. Choi and C. D. Montemagno, *Nano Lett.*, 2005, **5**, 2538–2542.
25 P. Broz, S. Driamov, J. Ziegler, N. Ben-Haim, S. Marsch, W. Meier and P. Hunziker, *Nano Lett.*, 2006, **6**, 2349–2353.
26 M. Nallani, O. Onaca, N. Gera, K. Hildenbrand, W. Hoheisel and U. Schwaneberg, *Biotechnol. J.*, 2006, **1**, 828–834.
27 D. M. Vriezema, J. Hoogboom, K. Velonia, K. Takazawa, P. C. M. Christianen, J. C. Maan, A. E. Rowan and R. J. M. Nolte, *Angew. Chem., Int. Ed.*, 2003, **42**, 772–776.
28 M. Nallani, H. M. de Hoog, J. J. L. M. Cornelissen, A. R. A. Palmans, J. C. M. van Hest and R. J. M. Nolte, *Biomacromolecules*, 2007, 3723–3728.
29 D. M. vriezema, P. M. L. Garcia, N. Sancho Oltra, N. S. Hatzakis, S. M. Kuiper, R. J. M. Nolte, A. E. Rowan and J. C. M. van Hest, *Angew. Chem., Int. Ed.*, 2007, 7378–7382.
30 P. C. J. Kamer, R. J. M. Nolte and W. Drenth, *J. Chem. Soc., Chem. Commun.*, 1986, 1789–1791.
31 J. C. M. van Hest, D. A. P. Delnoye, M. W. P. L. Baars, C. Elissen-Roman, M. H. P. van Genderen and E. W. Meijer, *Chem.–Eur. J.*, 1996, **2**, 1616–1626.
32 J. J. L. M. Cornelissen, M. Fischer, R. van Waes, R. van Heerbeek, P. C. J. Kamer, J. N. H. Reek, N. A. J. M. Sommerdijk and R. J. M. Nolte, *Polymer*, 2004, **45**, 7417–7430.
33 D. M. Vriezema, *PhD Thesis*, Radboud University Nijmegen, 2005, p. 195.
34 J. J. L. M. Cornelissen, M. Fischer, N. A. J. M. Sommerdijk and R. J. M. Nolte, *Science*, 1998, **280**, 1427–1430.
35 G. A. Metselaar, J. J. L. M. Cornelissen, A. E. Rowan and R. J. M. Nolte, *Angew. Chem., Int. Ed.*, 2005, **44**, 1990–1993.
36 J. J. L. M. Cornelissen, J. J. J. M. Donners, R. de Gelder, W. S. Graswinckel, G. A. Metselaar, A. E. Rowan, S. N. A. J. M. and R. J. M. Nolte, *Science*, 2001, **293**, 676–680.
37 J. J. L. M. Cornelissen, W. S. Graswinckel, A. E. Rowan, N. A. J. M. Sommerdijk and R. J. M. Nolte, *J. Polym. Sci., Part A: Polym. Chem.*, 2003, **41**, 1725–1736.
38 A. J. M. van Beijnen, R. J. M. Nolte, W. Drenth, A. M. F. Hezemans and P. J. F. M. van de Coolwijk, *Macromolecules*, 1980, **13**, 1386–1391.
39 A. J. M. van Beijnen, R. J. M. Nolte, A. J. Naaktgeboren, J. W. Zwikker, W. Drenth and A. M. F. Hezemans, *Macromolecules*, 1983, **16**, 1679–1689.
40 J. A. Schellma, *Acc. Chem. Res.*, 1968, **1**, 144-&.
41 W. Kuhn, *Trans. Faraday Soc.*, 1930, **26**, 293–308.
42 G. A. Metselaar, *PhD Thesis*, Radboud University, Nijmegen, 2006.
43 J. T. Huang, J. Sun, W. B. Euler and W. Rosen, *J. Polym. Sci., Part A: Polym. Chem.*, 1997, **35**, 439–446.
44 S. J. Wezenberg, G. A. Metselaar, A. E. Rowan, J. J. L. M. Cornelissen, D. Seebach and R. J. M. Nolte, *Chem.–Eur. J.*, 2006, **12**, 2778–2786.
45 R. J. M. Nolte, *Chem. Soc. Rev.*, 1994, **23**, 11–19.
46 R. J. M. Nolte, J. W. Zwikker, J. Reedijk and W. Drenth, *J. Mol.Catal.*, 1978, **4**, 423–426.
47 P. C. J. Kamer, R. J. M. Nolte and W. Drenth, *J. Am. Chem. Soc.*, 1988, **110**, 6818–6825.
48 B. Hong and M. A. Fox, *Macromolecules*, 1994, **27**, 5311–5317.
49 L. F. Beste and H. K. Hall, *J. Phys. Chem.*, 1964, **68**, 269–274.
50 C. Graf, W. Schartl, K. Fischer, N. Hugenberg and M. Schmidt, *Langmuir*, 1999, **15**, 6170–6180.
51 L. Zhang and A. Eisenberg, *J. Am. Chem. Soc.*, 1996, **118**, 3168–3181.
52 L. Zhang and A. Eisenberg, *J. Polym. Sci., Part B: Polym. Phys.*, 1999, **37**, 1469–1484.
53 A. T. Nikova, V. D. Gordon, G. Cristobal, M. R. Talingting, D. C. Bell, C. Evans, M. Joanicot, J. A. Zasadzinski and D. A. Weitz, *Macromolecules*, 2004, **37**, 2215–2218.
54 N. Ouarti, P. Viville, R. Lazzaroni, E. Minatti, M. Schappacher, A. Deffieux and R. Borsali, *Langmuir*, 2005, **21**, 1180–1186.
55 A. A. Choucair, A. H. Kycia and A. Eisenberg, *Langmuir*, 2003, **19**, 1001–1008.
56 D. M. Vriezema, A. Kros, R. de Gelder, J. J. L. M. Cornelissen, A. E. Rowan and R. J. M. Nolte, *Macromolecules*, 2004, **37**, 4736–4739.

